University of Pennsylvania
ScholarlyCommons

Departmental Papers (CBE)

Department of Chemical & Biomolecular Engineering

12-1-2007

Interaction of CO with Surface PdZn Alloys

Eseoghene Jeroro
University of Pennsylvania

V. Lebarbier
University of New Mexico

A. Datye
University of New Mexico

Y. Wang
Pacific Northwest National Laboratory

John M. Vohs
University of Pennsylvania, vohs@seas.upenn.edu

Postprint version. Published in *Surface Science*, Volume 601, Issue 23, December 2007, pages 5546-5554.
Publisher URL: http://dx.doi.org/10.1016/j.susc.2007.09.031

This paper is posted at ScholarlyCommons. http://repository.upenn.edu/cbe_papers/102
For more information, please contact repository@pobox.upenn.edu.

Interaction of CO with Surface PdZn Alloys

E. Jeroro[1], V. Lebarbier[2], A. Datye[2], Y. Wang[3] and J. M. Vohs[1]

[1]*Department of Chemical and Bimolecular Engineering, University of Pennsylvania, Philadelphia, PA 19104, USA*
[2]*Department of Chemical and Nuclear Engineering, University of New Mexico, Albuquerque, NM 87131, USA*
[3]*Pacific Northwest National Laboratory, Richland, WA 99352, USA*

ABSTRACT

The adsorption and bonding configuration of CO on clean and Zn-covered Pd(111) surfaces was studied using Low Energy Electron Diffraction (LEED), Temperature Programmed Desorption (TPD) and High Resolution Electron Energy Loss Spectroscopy (HREELS). LEED and TPD results indicate that annealing at 550 K is sufficient to induce reaction between adsorbed Zn atoms and the Pd(111) surface resulting in the formation of an ordered surface PdZn alloy. Carbon monoxide was found to bond more weakly to the Zn/Pd(111) alloy surfaces compared to clean Pd(111). Zn addition was also found to alter the preferred adsorption sites for CO from threefold hollow to atop sites. Similar behavior was observed for supported Pd-Zn/Al_2O_3 catalysts. The results of this study show that both ensemble and electronic effects play a role in how Zn alters the interactions of CO with the surface.

INTRODUCTION

The interest in using fuel cells as highly-efficient, energy conversion devices has motivated research in the development of methods for both hydrogen production and storage. Alcohols, such as methanol and ethanol, have been proposed as possible sources of hydrogen that can be easily stored and transported and have the added benefit of being potentially bio-renewable resources [1-5]. To use alcohols for this purpose, however, they must be easily reformed into H_2 and CO_2 and this requires highly active and stable reforming catalysts. The most studied catalyst for steam reforming of CH_3OH (SRM, $CH_3OH + H_2O \rightarrow CO_2 + 3H_2$) is Cu supported on ZnO [6-9]. While this catalyst is

highly active and selective, it has low stability from sintering and is pyrophoric once reduced. Pd supported on ZnO has been proposed as an alternative catalyst for SRM that does not suffer from some of the drawbacks of Cu/ZnO [10-17]. Iwasa et al. were the first to report that Pd/ZnO catalysts are active for SRM and that they exhibit an unusually high selectivity (>95%) for the production of CO_2 and H_2 from methanol [10,11,18]. This result is somewhat surprising in light of the fact that bulk Pd exhibits nearly 100% selectivity for the decomposition of CH_3OH to CO (rather than CO_2) and H_2 under typical SRM conditions [13]. Iwasa and others have also demonstrated that partial alloying of the Pd with Zn is required to obtain a highly selective Pd/ZnO SRM catalyst [12,16-19]. While the importance of alloy formation has been established, the mechanism by which Zn alters the selectivity to produce CO_2 rather than CO is not well understood.

In order to understand how alloying with Zn affects the reactivity of Pd we have recently reported on the studies of the reaction of CH_3OH on model catalysts consisting of Pd supported on a ZnO(0001) single crystal [20]. One observation in these studies was that alloying of the Pd with Zn provided by the ZnO(0001) surface alters both the dehydrogenation activity of the catalyst and the heat of adsorption of CO. This latter finding is consistent with a study by Rodriguez of the adsorption of CO on bulk PdZn alloy surfaces [21]. We have extended our studies of the reactivity of Pd/ZnO(0001) model catalysts to include the adsorption and reaction of both CO and methanol on Zn-covered Pd(111) surfaces. The results of our study of CO on Zn/Pd(111) are reported here and those for CH_3OH will be reported in a future publication.

While the interaction of CO with Zn/Pd(111) has not been studied in detail previously, there have been several previous studies of the structure of Zn-covered Pd(111) surfaces [22,23]. In the first such study Bayer et al. [22] used low energy electron diffraction (LEED) and photoelectron spectroscopy to characterize the structure and thermal stability of vapor-deposited Zn films, and the electronic interactions between Zn and Pd. Their LEED results showed that at 105 K vapor-deposited Zn grows in a layer-by-layer fashion forming a pseudomorphic overlayer on the Pd(111) surface. Using grazing emission x-ray photoelectron spectroscopy (XPS) they were able to distinguish between Zn adatoms and Zn atoms that had become incorporated into the Pd lattice. Using this data in conjunction with LEED results they showed that monolayer Zn films

reacted with the Pd(111) surface at temperatures above 300 K to form a PdZn alloy. Samples heated between at 550 and 600 K exhibited a p(2x1) LEED pattern indicating the formation of an ordered alloy with a Pd:Zn ratio of 1:1. Heating above 600 K resulted in dissolution of the Zn into the bulk of the Pd(111) sample.

In a subsequent study Gabasch et al. [23] also investigated the interaction of vapor-deposited Zn layers with Pd(111) using LEED and CO adsorption measurements. They concluded that between 300 and 400 K the Zn forms monolayer and then multilayer films but does not react with the Pd(111) surface to form an alloy. They also observed that upon heating multilayer Zn films from 400 to 600 K, all but the first layer of Zn desorbs. In this temperature range they again concluded that monolayer Zn films do not react with the Pd(111) surface to form an alloy. Monolayer Zn, however, was found to diffuse into the Pd upon heating above 650 K. They also report observing a p(2x2) LEED pattern that was sharpest for a 0.75 ML Zn film that was annealed at 550 K. They interpreted this LEED pattern to be due to the formation of a p(2x2)-3Zn surface adlayer.

Obviously, the Gabasch et al. [23] model of the structure of monolayer Zn films on Pd(111) is in conflict with that of Bayer et al.[22] with the biggest disagreement being whether between 300 and 600 K Zn monolayers merely form ordered overlayers or react with the Pd surface to form an ordered surface alloy. It should be noted that many of Gabasch et al. conclusions about the surface Zn coverage are based on analysis of CO TPD measurements in which they have assumed that there is a one-to-one correspondence between the number of exposed Pd atoms and the CO uptake. The results of the present study will show that this is not a valid assumption and that the preferred CO adsorption site (threefold hollow, twofold bridging, or atop) is affected by the presence of Zn on the Pd(111) surface. Adsorbed Zn can also cause the CO desorption temperature to be lower than 300 K which is below the temperature at which Gabasch et al. did their CO uptake experiments. These observations cast some doubt on the method used by Gabasch et al. to measure the amount of exposed Pd on the surface and consequently their conclusion that only ordered Zn adlayers are formed between 300 and 600 K rather than a PdZn alloy is also questionable. As will be discussed in detail below, our results are consistent with those of the Bayer study [22] and support the formation of an ordered surface PdZn alloy upon heating submonolayer and monolayer

films on Pd(111) to temperatures between 300 and 600 K. In addition to helping clarify the structure of Zn films on Pd(111) and their reaction with the support to form ordered alloy structures, the results of this study provide new insight into the effect of the incorporation of Zn into the Pd(111) surface on the adsorption sites and bonding of CO.

MATERIALS AND METHODS

The experiments were carried out in an ultra high vacuum (UHV) chamber with a background pressure of 2 x 10^{-10} Torr. The chamber was equipped with an ion sputter gun for sample cleaning, a quadrupole mass spectrometer (UTI) for Temperature Programmed Desorption (TPD) studies, a quartz crystal film thickness monitor (Maxtek Inc.) for monitoring the flux from the zinc metal deposition source, a retarding field electron energy analyzer (OCI Vacuum Microengineering) that was used for Low Energy Electron Diffraction (LEED), and a High Resolution Electron Energy Loss (HREEL) spectrometer (LK Technologies). The HREELS experiments were performed with incident electron beam energy of 4 eV directed 60º from the normal and a resolution of 4 – 5 meV of the elastically scattered peak.

The Pd(111) single crystal used in this study was 10 mm x 5mm x 1mm in size. The sample temperature was measured using a chromel–alumel thermocouple that was spot-welded onto the back of the sample. The sample was cleaned using repeated cycles of 2 kV argon ion bombardment, followed by annealing in a vacuum at 1150 K for 20 s. The absence of impurities on the sample surface was confirmed using a combination of HREELS, LEED, and TPD. Cooling of the sample to 100 K was done using liquid nitrogen.

Zn was deposited onto the Pd(111) surface using an evaporative Zn source consisting of a short length of 0.5 mm diameter, high-purity Zn wire wrapped around a 0.2 mm diameter tungsten filament. The tungsten filament was attached to an electrical feedthrough on the UHV system and heated resistively. The Zn flux from the source was monitored using the quartz crystal film thickness monitor. We report Zn coverages as effective monolayers where one monolayer was assumed to be of 1.53 x 10^{15} atoms/cm^2 which is the density of Pd atoms on the Pd(111) surface.

The CO adsorbate (99.99 % Sigma-Aldrich) used in this study was introduced into the chamber through a variable leak valve that was attached to a 5 mm stainless steel dosing needle. The sample was positioned in front of the dosing needle during CO exposure. A heating rate of 3 K/s was used in the TPD experiments.

For comparison purposes, Fourier-transform infrared (FTIR) spectra of the interaction of CO with a high surface area $Pd/ZnO/Al_2O_3$ catalyst were also collected. The $Pd/ZnO/Al_2O_3$ catalyst used in these studies was prepared by incipient wetness impregnation into an Al_3O_3 support (boehmite calcined at 1125 K for 5h) using solutions of Pd and Zn nitrate (Pd/Zn molar ratio = 0.38). The catalyst was pressed into a pellet for FTIR analysis and spectra were collected using a Nicolet Magna 750 spectrometer equipped with a mercury cadmium telluride detector (4 cm^{-1} resolution, 128 scans).

RESULTS AND DISCUSSION

Structure of Zn/Pd(111) surfaces

As described in the experimental section, Zn films were deposited using an evaporative Zn source with the Pd(111) sample held at 300 K and the Zn coverage was determined using a quartz crystal film thickness monitor. Following each deposition the sample was annealed for 2 mins at 550 K. Based on the results of the study by Bayer et al. [22], this temperature is sufficient to induce reaction of the Zn adlayer with the substrate to form an ordered PdZn alloy surface, but low enough to prevent dissolution of the Zn into the bulk of the crystal. LEED was used to characterize the structure of the PdZn alloy surfaces produced in this manner. Figure 1 displays LEED patterns obtained using a 50 eV electron beam as a function of the Zn coverage. Pattern (a) in this figure is for the clean Pd(111) surface and consists of a sharp (1x1) hexagonal pattern. Pattern (b) corresponds to a 0.25 ML Zn/Pd(111) sample which had been annealed at 550 K. This pattern is more complex than that of the clean surface and is best described as a p(2x2) structure. Note that the spots in this pattern are more diffuse than those in the pattern for the clean surface indicating some disorder in the surface layer. Pattern (c) corresponds to a 0.5 ML Zn/Pd(111) sample and exhibits a p(2x1) structure. This result is consistent

with that reported by Bayer et al. [22] who also observed ordered p(2x1) superstructures for 1 ML Zn/Pd samples heated between 450 and 600 K.

Our LEED results in conjunction with both the LEED and XPS results of Bayer et al. [22] indicate that the structure of the Zn/Pd(111) surfaces that have been heated sufficiently to induce alloy formation evolve with Zn coverage as shown in Figure 2. Part (a) of this figure depicts the hexagonal lattice of the clean Pd(111) surface, while Part (d) shows the structure of the p(2x1)-PdZn(111) alloy surface. Note the 1:1 Pd:Zn stoichiometry of the p(2x1) surface is consistent with the observation that this pattern emerges at a Zn coverage of 0.5 ML. A p(2x2) PdZn alloy surface with a 4:1 Pd:Zn stoichiometry is displayed in Figure 2c. While LEED patterns distinct from the substrate could not be obtained for Zn coverages less than 0.25 ML, the results for higher coverages allow us to predict the structures for low Zn coverages. For example Figure 2b shows the expected p(4x4) structure for a 0.06 ML Zn/Pd(111) sample.

CO on Pd(111)

To provide base case data for comparison to the Zn-covered surfaces, the interaction of CO with clean Pd(111) was initially characterized using TPD and HREELS. Figures 3 and 4 display CO TPD data and the C-O stretching region of the HREEL spectra, respectively, as a function of the CO dose. In this set of experiments the CO dose was varied from 0 to 300 L. Only the spectra obtained for doses of 0.5, 50 and 100 L of CO are shown in the figure. Note that the sloping background in the 50 and 100 L runs is due to a decrease in the background pressure of CO during the duration of the TPD experiments. For doses up to 0.5 L, CO desorbs in a single peak centered at 460 K. Increasing the CO dose caused a shoulder to appear on the low-temperature side of the primary CO desorption peak in the TPD data indicating the presence of more than one adsorption site for CO on Pd(111). The position of this shoulder moved to lower temperatures with increasing CO exposures and is centered near 400 and 320 K for the 50 and 100 L CO doses, respectively. TPD data for CO doses between 100 and 300 L were nearly identical to those obtained for the 100 L CO dose indicating that this dose is sufficient to saturate the surface.

The HREELS data for the C-O stretching region in Figure 4 allows the bonding configuration of CO on the Pd(111) surface to be determined. For the sample exposed to 0.5 L of CO a single C-O stretching peak centered at 1860 cm^{-1} is observed. A second peak centered at 2090 cm^{-1} grows in with increasing CO coverage. The data in Figures 3 and 4 are consistent with the literature where it has been reported that for low CO coverages on Pd(111), CO adsorbs carbon-end down in threefold hollow sites as illustrated in Figure 4 [24,25]. The C-O stretching frequency for this threefold CO is approximately 1850 cm^{-1} [24,25] and this bonding site saturates at a CO coverage of 1/3 ML [25,26]. Desorption of this specie gives rise to the peak at 460 K in the TPD spectrum. Increasing the CO coverage results in compression of the CO layer and above 300 K the population of both twofold bridging and atop sites. Below 150 K only the threefold and atop species are observed [25]. The peak at 2090 cm^{-1} can be assigned to the atop specie in accordance with the literature. A high coverage of CO adsorbed in the twofold bridging sites can be obtained by dosing CO at 300 K [25,27,28]. This is illustrated by the HREEL data presented in Figure 5 which was obtained for various CO doses at 300 K. Note that for high coverages the spectrum contains a single peak centered at 1910 cm^{-1} which corresponds to the bridge-bound species [25]. It is not possible to identify distinct peaks for CO adsorbed in twofold-bridge and atop sites in the TPD data in Figure 3, but these species give rise to the broad desorption feature between 230 and 380 K for the sample dosed with 100 L of CO. The low-temperature portion of this feature is most likely primarily due to CO adsorbed in atop sites.

CO on Zn/Pd(111)

TPD data obtained from 550 K-annealed Zn/Pd(111) samples exposed to 0.5 L of CO for Zn coverages between 0 and 1 ML are shown in Figure 6. The 0.5 L CO dose was chosen based on the TPD results obtained from the clean Pd(111) surface which showed that it was sufficient to saturate the threefold sites. The two most obvious trends in this data are decreases in both the amount of adsorbed CO and the CO desorption temperature with increasing Zn coverage. The total amount of adsorbed CO as a function of the Zn coverage is plotted in Figure 7 and decreases from 1/3 ML for the clean

Pd(111) surface to 0 for the 1.0 ML Zn/Pd(111) sample. Note the non-linear shape of this curve.

HREELS was also used to characterize adsorbed CO on Zn/Pd(111). The C-O stretching region of HREEL spectra obtained from Zn/Pd(111) samples as a function of the Zn coverage are displayed in Figure 8. These spectra were collected at a sample temperature of 100 K following a 0.5 L dose of CO. As with the TPD data several prominent trends are apparent in the HREEL data. First the intensity of the C-O stretching peaks decrease with increasing Zn coverage. This result is consistent with the TPD results and shows that the amount of adsorbed CO decreases with the addition of Zn. The second trend apparent in the data is that the preferred bonding configuration for CO gradually changes from threefold hollow sites on the clean surface, to atop sites on the 0.8 and 0.5 ML Zn/Pd(111) samples. Bonding in both threefold and atop sites and possibly some bridging sites is observed for samples with intermediate Zn coverages.

Before delving into the fine details of the TPD and HREELS results, it is useful to compare the overall trends observed in these results to those reported previously for both Zn/Pd(111) and PdZn/Ru(001) model catalysts [21-23]. As noted in the introduction there is some controversy as to whether at temperatures between 300 and 600 K Zn merely forms ordered adlayers on Pd(111) or reacts with the surface to form an ordered alloy where Zn is substituted into the Pd lattice. Bayer et al. have argued for the latter based on XPS results [22], while Gabasch et al. have argued for the former based in large part on measurements of the number of exposed Pd atoms using CO TPD [23]. First it should be noted that the trends in the TPD data in Figure 6 are very similar to those obtained by Rodriquez for bulk PdZn alloys where it was also observed that the CO peak temperature decreases with increasing Zn concentration and approaches a limiting value of ~220 K [21]. While not conclusive, this similarity supports alloy formation.

One of Gabasch et al. arguments in favor of the formation of only Zn adlayers on the surface was based on their observation of a linear decrease in the amount of CO adsorbed with Zn coverage for samples annealed at 373 K [23]. They argued that if Zn reacted with the Pd and became incorporated into the near surface region as proposed by Bayer, a much slower decrease in the CO uptake should be observed since the migration of Zn into the sample would expose additional Pd adsorption sites on the surface. The

TPD and HREELS data obtained in this study demonstrate several problems with this argument. First Gabasch et al. observed a linear CO uptake versus Zn coverage relationship for samples that were dosed with CO at 300 K. The TPD data in Figure 6 show, however, that for Zn coverages as low as 0.1 ML a significant fraction of the CO desorbs below room temperature. Thus, Gabasch et al. may not have counted all the CO adsorption sites in their study. A second and perhaps more serious problem is illustrated by the HREELS results in Figure 8. As noted above, these data show that the preferred bonding site for CO changes from threefold hollow to atop upon Zn addition. For surfaces covered with 0.5 and 0.8 ML of Zn, the HREELS results show that the majority of the CO bonds in atop sites. As will be discussed in detail below, this result can be explained in part by the lack of threefold hollow sites that contain only Pd atoms for these Zn coverages. This change in the preferred CO bonding site makes it difficult to derive structural information from a plot of the amount of CO adsorbed versus Zn coverage. Our TPD data for Zn coverages of 0.5 and 0.8 ML, in conjunction with the HREELS results, however, do provide some insight into whether upon heating to 550 K the Zn remains as an adlayer or becomes incorporated into the near surface region of the Pd(111) sample. For these two Zn coverages, CO bonds almost exclusively in atop sites as shown by HREELS and thus changes in the bonding configuration do not significantly complicate the CO uptake analysis. As shown in Figure 6, the amount of CO adsorbed for a 0.5 L dose on the 0.5 and 0.8 ML Zn/Pd(111) samples was nearly constant. While the possibility that the CO sticking coefficient changes with Zn coverage needs to be taken into account, at least in this coverage regime, the addition of more Zn appears not to decrease the number of exposed Pd atoms. This result is consistent with Bayer et al. conclusion that for samples heated between 300 and 600 K the Zn reacts with the Pd to form an ordered surface PdZn alloy with a 1:1 stoichiometry [22].

Consistent with the previous studies of Zn/Pd(111), the amount of CO that adsorbed decreased to zero for a Zn coverage of 1 ML. This result appears to support Gabasch et al. model in which Zn remains as an adlayer on the surface. Note, however, that if alloy formation occurs, for this coverage there may be Zn present in both the first and second layers of the surface. Since, as will be discussed in detail below, Zn nearest neighbors destabilizes the interaction of CO with exposed Pd atoms, it is possible that for

high Zn coverages the CO desorption temperature is below 100 K, which was the lowest obtainable temperature in the present study. Rodriquez's study of the interaction of CO on PdZn alloy films provides some support for this argument [21]. In that study for high Zn to Pd ratios a CO desorption peak near 100 K was observed.

Examining the TPD results in more detail reveals that even very small amounts of Zn affect the bonding of CO on Pd(111). For example, incorporation of only 0.03 ML of Zn into the Pd(111) surface caused a significant decrease in the CO desorption temperature. For clean Pd(111) the 0.5 L CO dose saturates the threefold sites at a coverage of 1/3 ML. This threefold bound CO desorbs in a single peak centered at 460 K (see Figure 3). In contrast, for 0.03 ML Zn/Pd(111), the corresponding CO TPD curve contains a broad feature consisting of two overlapping peaks centered at 380 and 440 K. The HREELS data in Figure 8 show for this sample at 100 K, CO adsorbs primarily in threefold (1835 cm^{-1}) and atop sites (2090 cm^{-1}). The peak at 1835 cm^{-1} corresponding to three-fold hollow CO contains a shoulder on the high wavenumber side suggesting the presence of some bridge-bound species as well. Addition of another 0.03 ML of Zn for a total Zn coverage of 0.06 ML produced an even larger shift in the CO desorption peaks to lower temperatures. For this sample, CO desorbed in what appears to be several overlapping peaks centered between 280 and 400 K, with the highest-temperature peak being centered at 400 K. The HREEL spectra show a slight increase in the amount of atop CO relative to threefold and bridge species on the 0.06 ML Zn sample compared to the 0.03 ML sample. The HREELS results also show a decrease in the relative intensity at 1910 cm^{-1}, corresponding to bridge bound CO to that at 1835 cm^{-1} corresponding to threefold CO. Another difference in the HREEL spectra for the 0.03 and 0.06 Zn coverages is a downward shift in the peak position of the ν(CO) mode for the atop species from 2090 to 2030 cm^{-1}.

Assuming that the highest temperature feature in the TPD data for the 0.06 ML Zn sample corresponds to threefold CO, these results show that the incorporation of 0.06 ML of Zn in the surface causes the desorption temperature of this specie to decrease by 60 K. This roughly corresponds to a 16 kJ/mole decrease in the heat of adsorption of CO. When evaluating the influence of alloy formation on adsorption, one needs to consider both ensemble and electronic effects. The former refers to a change in the composition of

the adsorption site. An example of this would be replacing one of the Pd atoms in a threefold site with a Zn atom. The latter refers to a change in the electronic properties of the site due to interactions of the atoms that constitute the site with their nearest or next nearest neighbors. For the Zn/Pd(111) system there is clearly an ensemble effect, since Zn incorporation into the surface decreases the amount of CO that adsorbs in threefold sites. This result indicates that CO has a very low heat of adsorption on threefold sites that include one or two Zn atoms. As will be discussed below, this conclusion is consistent with DFT calculations of the energetics of the adsorption of CO on PdZn alloy surface [29,30,31].

In addition to the obvious ensemble effect, Zn incorporated into the Pd(111) surface also appears to have a large electronic effect that alters the bonding of CO on nearby Pd-only sites. This can be illustrated by considering the TPD results along with the model of the 0.06 ML Zn, p(4x4) PdZn(111) surface shown in Figure 2b. If one assumes that CO only adsorbs on threefold sites composed of three Pd atoms and not on those containing Zn, there are the following types of threefold sites on this surface: (1) one Pd with a Zn nearest neighbor, (2) two Pd with Zn nearest neighbors and (3) the Pd have no Zn nearest neighbors (these sites are indicated in figure 9). The type (3) sites are the most "Pd(111) like" and would be expected to be the most stable bonding sites for CO. Assuming this is the case, the TPD results show that CO bound in these sites is destabilized relative to threefold sites on Pd(111) by ~16 kJ/mole. Thus, nearby Zn has a strong electronic effect and influences bonding in Pd sites in which the Pd atoms only have Zn atoms as next nearest neighbors. Recent DFT calculations by Chen et al. for PdZn alloys provide insight into these electronic effects. Their calculations show that alloying Pd with Zn causes the Pd 4d valence band to shift to higher energy compared to bulk Pd [29,30]. This shift has also been observed experimentally for surface PdZn alloys on Pd(111) by Bayer et al. [22] using ultraviolet photoelectron spectroscopy.

Increasing the Zn coverage to 0.1 ML caused a further broadening of the CO desorption signal and for this sample, CO desorbed in multiple overlapping features between 320 and 450 K. The HREELS data (Figure 8) shows that for this surface at 100 K, there are nearly equal amounts of CO adsorbed in threefold hollow and atop sites. The atop species are the weaker bound of the two and mostly desorb between 200 and 300 K.

This is demonstrated by the HREEL data in Figure 10 which shows the C-O stretching region for the CO-dosed, 0.10 ML Zn/Pd(111) sample at 100 K and after heating to 380 K. As noted earlier, at 100 K the peaks for the threefold and atop species are of equal intensity. Heating to 380 K, however, caused the intensity of the atop peak at 2090 cm^{-1} to decrease significantly. Upon heating some broadening is also observed in the peak at 1835 cm^{-1} due to the threefold CO and a shoulder near 1910 cm^{-1} emerges. This latter peak position corresponds to twofold bridge-bound CO. This result is consistent with that reported by Kuhn et al. [25] who showed that for Pd(111) under equilibrium adsorption conditions bridge-bound CO is not preferred below ~150 K.

The TPD curve for the 0.25 ML Zn/Pd(111) sample contains a sharp desorption peak at 250 K and a series of smaller overlapping peaks at higher temperatures extending up to ~400 K. The model of the p(2x2) 0.25 ML Zn/Pd(111) surface in Figure 2c shows that there is only one type of Pd-only threefold hollow site on this surface in which each Pd atom has 2 Zn nearest neighbors. This in conjunction with the continued decrease in both the maximum CO desorption temperature and the intensity of the high-temperature portion of the CO desorption spectrum further demonstrates that Zn nearest neighbors destabilize the bonding of CO in the threefold sites.

As shown in Figure 2, on the p(2x1) surfaces produced by annealing the 0.5 and 0.8 ML Zn/Pd(111) samples to 550 K there are no threefold sites composed only of Pd atoms. The TPD data for these samples contain a single CO desorption feature centered at 230 K and the HREEL spectrum is dominated by the peak at 2030 cm^{-1} corresponding to atop CO. The total amount of CO that adsorbs on these surfaces is also significantly less than that for the lower Zn coverage samples. These results show that on the p(2x1) surface, CO adsorbs only atop the exposed Pd atoms and further demonstrate that CO does not bond directly to the surface Zn atoms for temperatures above 100 K.

It is interesting to compare the experimental results obtained in this study for the p(2x1) 0.5 ML Zn/Pd(111) alloy surface to the theoretical calculations of Chen et al. [29,30] who used DFT to estimate the adsorption energies of CO on the various sites on a PdZn(111) alloy surface (this surface has the same structure as that of the p(2x1) Zn/Pd(111) surface). Consistent with the experimental results in this and previous studies [21] their calculations showed that CO interacts much more weakly with Zn sites

compared to Pd sites. They studied the interaction of CO with the two possible threefold hollow sites on the PdZn(111) surface. One of these sites is composed of two Pd atoms and one Zn atom and the other contains two Zn atoms and one Pd atom. During geometry optimizations they found that for both sites the CO drifted to either Pd atop sites or bridging sites between two Pd atoms. Their calculated heats of adsorption on the Pd atop and bridge sties were found to be equal. This result is consistent with the present study which shows that CO prefers the Pd atop sites on the p(2x1) Zn/Pd(111) alloy surface. Chen et al. calculations also predicted a C-O vibrational frequency of 2026 cm^{-1} for CO adsorbed in atop Pd sites. This value is essentially identical to the experimental value obtained here.

Finally, it is useful to consider whether the results obtained in this study provide useful insight into the effect of Zn incorporation into Pd on the interaction of CO with high surface area catalysts. In order to allow such connections to be made between the model and real world catalysts we have also used FTIR to study the interaction of CO with $Pd/ZnO/Al_2O_3$ catalysts. While a detailed description of these studies of high surface area catalysts will be presented in a future publication, it is worthwhile to note that many of the effects of Zn observed in the present study appear to also be important in real catalysts. For example, Figure 11 displays FTIR spectra collected at room temperature of the CO stretching region of two separate $Pd/ZnO/Al_2O_3$ catalysts which have been exposed to CO. Spectrum A in the figure corresponds to a catalyst reduced in H_2 at room temperature such that all the Pd is present as Pd metal (i.e. this sample does not contain any PdZn alloy). The IR spectrum contains a large peak at 1980 cm^{-1} and a smaller peak at 2062 cm^{-1} which are indicative of CO adsorbed in bridging and atop sites on the Pd, respectively. A broad tail on the 1980 cm^{-1} peak that extends beyond 1800 cm^{-1} is also readily apparent suggesting the presence of a significant amount of CO in threefold sites. Spectrum B in the figure was obtained from a $Pd/ZnO/Al_2O_3$ catalyst that was reduced in H_2 at 773 K. In this sample all of the Pd was present in the form of a PdZn alloy as determined by XRD. Note that for this sample the FTIR spectrum of adsorbed CO is dominated by a peak at 2070 cm^{-1} corresponding to atop bonded CO. Very little bridging or threefold CO is present on this sample. Thus, just as was the case for the model single crystal catalysts, for the high surface area catalyst, incorporation of

Zn into the Pd caused a change in the preferential bonding configuration of CO from threefold and bridging to atop. Furthermore, this result suggests that the single crystal catalysts provide a good model system for studying the effect of alloying Pd with Zn on surface reactivity.

CONCLUSIONS

The LEED and CO TPD results obtained in this study show that vapor deposited Zn reacts with the Pd(111) surface upon heating to 550 K to form an ordered surface PdZn alloy. This result is consistent with that reported previously by Bayer et al. [22]. The incorporation of Zn into the Pd(111) surface and the formation of the surface alloy was found to have a significant effect on the adsorption and bonding of CO. Carbon monoxide interacts only weakly with exposed Zn atoms on the alloy surface and at temperatures above 100 K does not adsorb on sites that contain Zn. In addition to this ensemble effect, Zn also has a strong electronic effect and destabilizes the bonding of CO on nearby Pd-only sites. For example, the heat of adsorption of CO was destabilized by ~16 kJ/mol on threefold Pd sites that have Zn next nearest neighbors compared to threefold sites on the clean Pd(111) surface. Finally, the HREELS results obtained in this study show that Zn incorporation into the Pd(111) surface shifts the preferred bonding configuration of CO on Pd(111) from threefold hollow and bridge sites to atop sites. These results are not only consistent with DFT calculations which show that CO prefers Pd atop sites on the p(2x1) Zn/Pd(111) alloy surface, but also with the FTIR results on high surface area catalysts.

ACKNOWLEDGEMENTS

Funding for this study was provided by the U.S. Department of Energy (grant no. DE-FG02-05ER15712 and DE-FG02-04ER15605).

REFERENCES

[1] J.C. Amphlett, K.A.M. Creber, J.M. Davis, R.F. Mann, B.A. Peppley, D.M. Stokes, Int. J. Hydrogen Energ. 19 (1994) 131.

[2] J.C. Amphlett, M.J. Evans, R.A. Jones, R.F. Mann, R.D. Weir, Can. J. Chem. Eng. 59 (1981) 720.

[3] J.C. Amphlett, M.J. Evans, R.F. Mann, R.D. Weir, Can. J. Chem. Eng. 63 (1985) 605.

[4] B. Wahlund, J.Y. Yan, M. Westermark, Biomass Bioenerg. 26 (2004) 531.

[5] G.A. Deluga, J.R. Salge, L.D. Schmidt, X.E. Verykios, Science 303 (2004) 993.

[6] L.C. Wang, Y.M. Liu, Y. Cao, G.S. Wu, C.Z. Yao, W.L. Dai, H.Y. He, K.N. Fan, Acta Chim. Sinica 65 (2007) 173.

[7] L.C. Wang, Y.M. Liu, M. Chen, Y. Cao, H.Y. He, G.S. Wu, W.L. Dai, K.N. Fan, J. Catal. 246 (2007) 193.

[8] S. Fukahori, T. Kitaoka, A. Tomoda, R. Suzuki, H. Wariishi, Appl. Catal. A-Gen. 300 (2006) 155.

[9] T. Shishido, Y. Yamamoto, H. Morioka, K. Takaki, K. Takehira, Appl. Catal. A-Gen. 263 (2004) 249.

[10] N. Iwasa, T. Mayanagi, S. Masuda, N. Takezawa, React. Kinet. Catal. L. 69 (2000) 355.

[11] N. Iwasa, W. Nomura, T. Mayanagi, S. Fujita, M. Arai, N. Takezawa, J. Chem. Eng. Jpn. 37 (2004) 286.

[12] N. Iwasa, N. Ogawa, S. Masuda, N. Takezawa, B. Chem. Soc. Jpn. 71 (1998) 1451.

[13] N. Takezawa, N. Iwasa, Catal. Today 36 (1997) 45.

[14] Y.H. Chin, R. Dagle, J.L. Hu, A.C. Dohnalkova, Y. Wang, Catal. Today 77 (2002) 79.

[15] Y.H. Chin, Y. Wang, R.A. Dagle, X.H.S. Li, Fuel Process. Technol. 83 (2003) 193.

[16] Y.H. Wang, J.C. Zhang, H.Y. Xu, X.F. Bai, Chinese J. Catal. 28 (2007) 234.

[17] Y.H. Wang, J.C. Zhang, H.Y. Xu, Chinese J. Catal. 27 (2006) 217.
[18] N. Iwasa, S. Masuda, N. Ogawa, N. Takezawa, Appl. Catal. A-Gen. 125 (1995) 145.
[19] A. Karim, T. Conant, A. Datye, J. Catal. 243 (2006) 420.
[20] P. Bera, J.M. Vohs, J. Phys. Chem. C 111 (2007) 7049.
[21] J.A. Rodriguez, J. Phys. Chem. 98 (1994) 5758.
[22] A. Bayer, K. Flechtner, R. Denecke, H.P. Steinruck, K.M. Neyman, N. Rosch, Surf. Sci. 600 (2006) 78.
[23] H. Gabasch, A. Knop-Gericke, R. Schlogl, S. Penner, B. Jenewein, K. Hayek, B. Klotzer, J. Phys. Chem. B. 110 (2006) 11391.
[24] X.C. Guo, J.T. Yates, J. Chem. Phys. 90 (1989) 6761.
[25] W.K. Kuhn, J. Szanyi, D.W. Goodman, Surf. Sci. 274 (1992) L611.
[26] P. Sautet, M.K. Rose, J.C. Dunphy, S. Behler, M. Salmeron, Surf. Sci. 453 (2000) 25.
[27] G. Rupprechter, V.V. Kaichev, H. Unterhalt, A. Morkel, V.I. Bukhtiyarov, Appl. Surf. Sci. 235 (2004) 26.
[28] G. Rupprechter, H. Unterhalt, M. Morkel, P. Galletto, T. Dellwig, H.J. Freund, Vacuum 71 (2003) 83.
[29] Z.X. Chen, K.M. Neyman, K.H. Lim, N. Rosch, Langmuir 20 (2004) 8068.
[30] Z.X. Chen, K.M. Neyman, A.B. Gordienko, N. Rosch, Phys. Rev. B 68 (2003).
[31] K.M. Neyman, R. Sahnoun, C. Inntam, S. Hengrasmee, N. Rosch, J. Phys. Chem. B 108 (2004) 5424.

FIGURE CAPTIONS

Figure 1. LEED patterns obtained at a beam energy of 50 eV for (a) clean Pd(111) (b) 0.25 ML Zn/Pd(111) annealed to 550 K, and (c) 0.5 ML Zn/Pd(111) annealed to 550 K.

Figure 2. Structural models of (a) clean Pd(111), (b) 0.06 ML Zn/Pd(111), (c) 0.25 ML Zn/Pd(111), and (d) 0.5 ML Zn/Pd(111).

Figure 3. CO TPD from Pd(111) as a function of coverage. CO was dosed at a sample temperature of 100 K.

Figure 4. HREEL spectra of CO on Pd(111) at 100 K as a function of coverage.

.

Figure 5. HREEL spectra of CO on Pd(111) at 300 K as a function of coverage.

Figure 6. CO TPD from Zn/Pd(111) that had been annealed at 550 K as a function of the Zn coverage. A 0.5 L CO dose was used in each TPD run.

Figure 7. The total amount of adsorbed CO on the Zn/Pd(111) sample for a 0.5 L CO doses as a function of the Zn coverage.

Figure 8. HREEL spectra obtained following exposure of the Zn/Pd(111) sample to 0.5 L of CO at 100 K as a function of the Zn coverage.

Figure 9. Model of 0.06 ML of Zn/Pd alloy surface showing the three different types of three-fold hollow sites: (1) one Pd with a Zn nearest neighbor, (2) two Pd with Zn nearest neighbors and (3) no Pd with Zn next nearest neighbors.

Figure 10. HREEL spectra 0.1 ML Zn/Pd(111) sample dosed with 0.5 L of CO at 100 K and after heating to 380 K.

Figure 11. FTIR spectra of CO adsorbed on (A) $Pd/ZnO/Al_2O_3$, and (B) $PdZn/ZnO/Al_2O_3$. The spectra were collected at a sample temperature of 293 K.

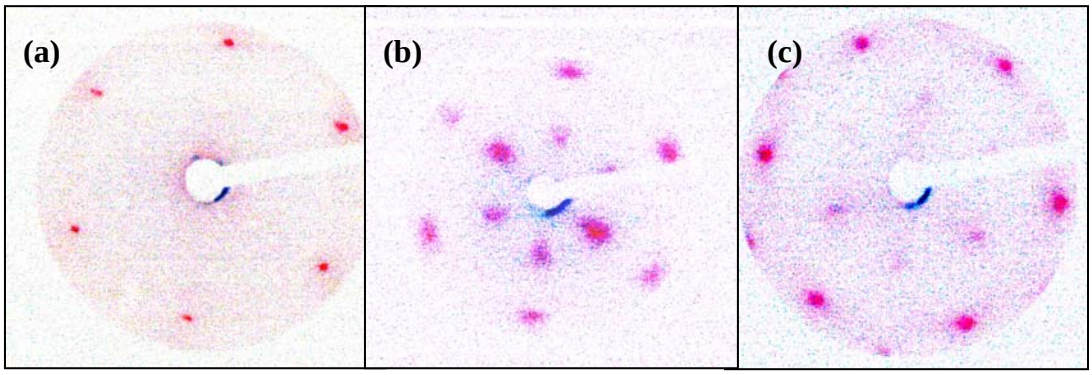

Figure 1. LEED patterns obtained at a beam energy of 50 eV for (A) Clean Pd(111) surface (B) 0.25 ML Zn / Pd closely resembling a p(2x2) structure and (c) 0.5 ML Zn / Pd showing a p(2x1) structure

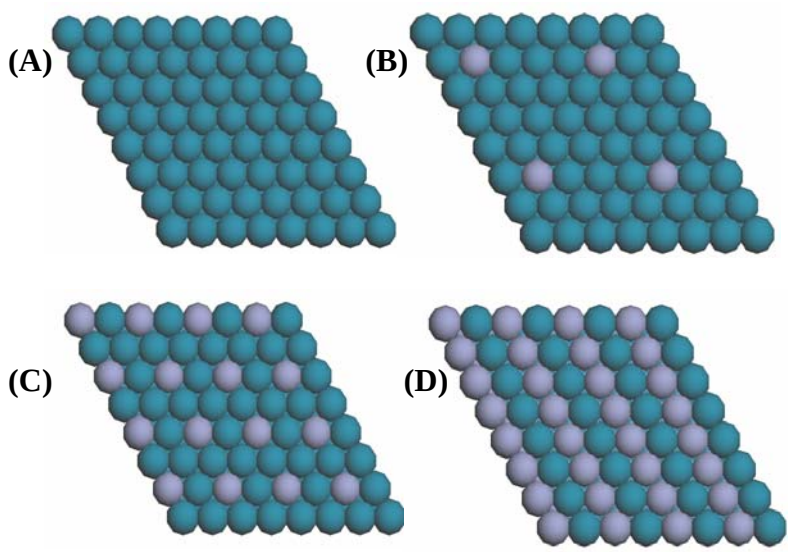

Figure 2.Models showing the crystal structure of the (A) Clean Pd(111) (B) 0.06 ML of Zn (C) 0.25 ML of Zn (D) 0.5 ML of Zn surface after alloy formation.

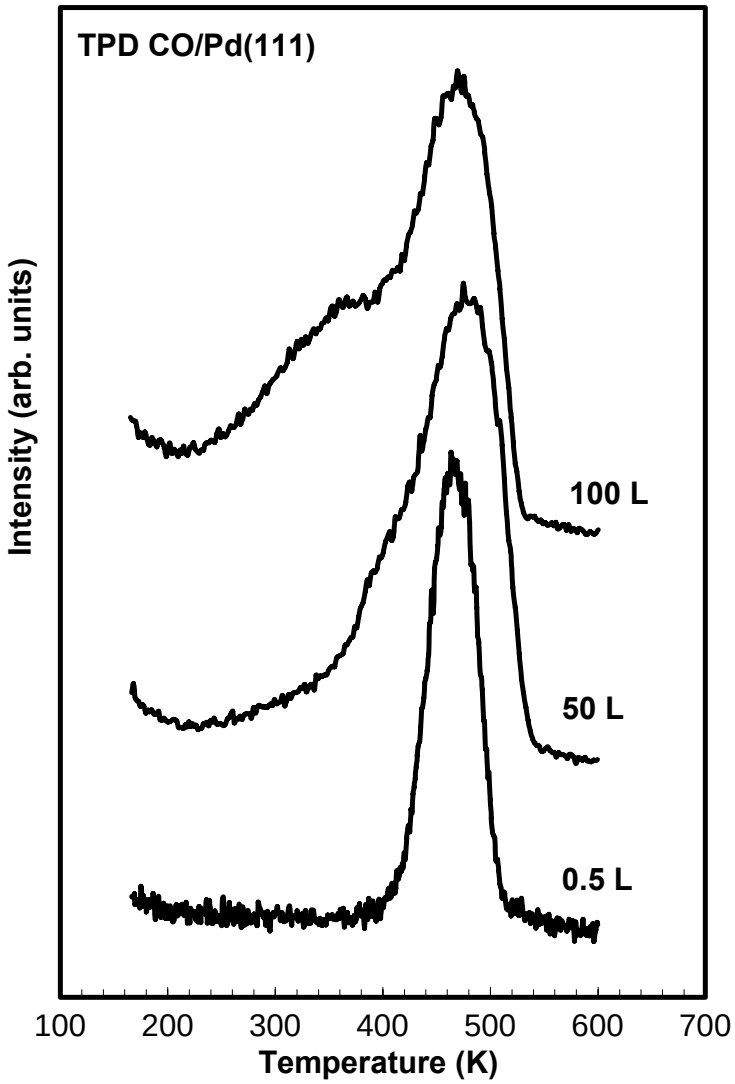

Figure 3. TPD data obtained after dosing different coverages of CO on Pd(111) at 100 K

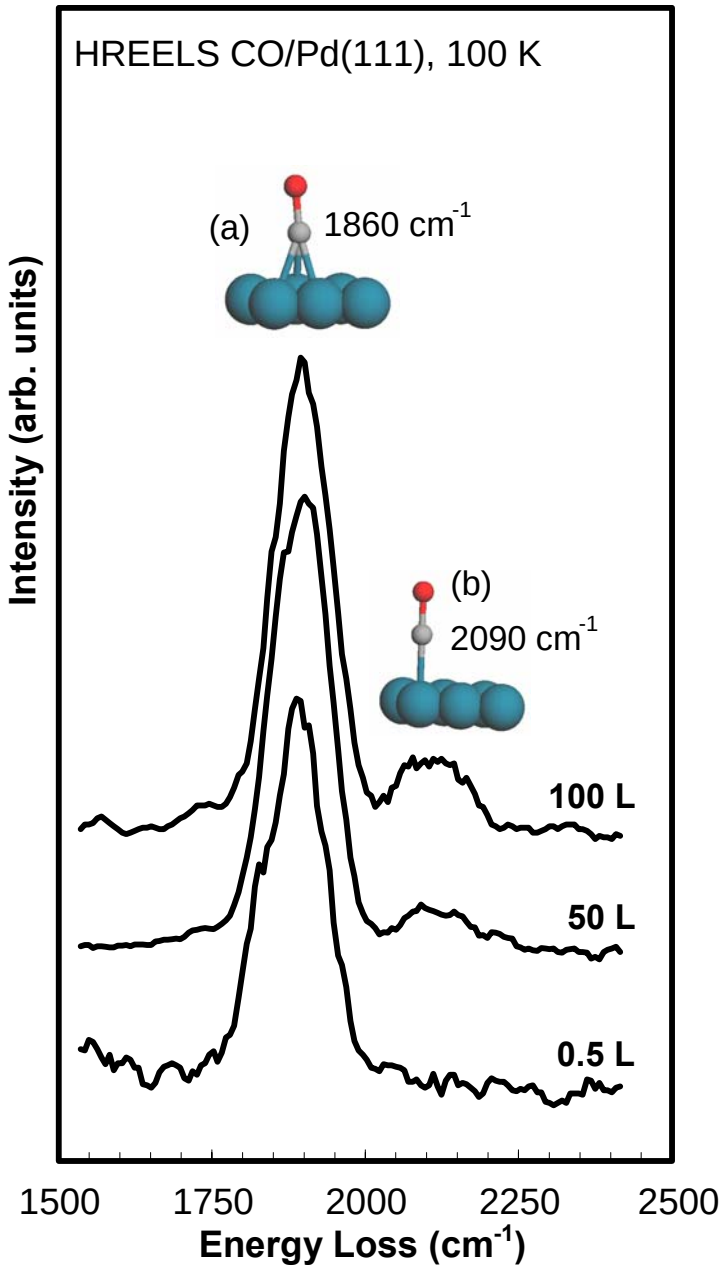

Figure 4. HREEL Spectra obtained after dosing different coverages of CO on Pd(111) at 100 K showing CO adsorbed on (a) three-fold hollow and (b) atop sites

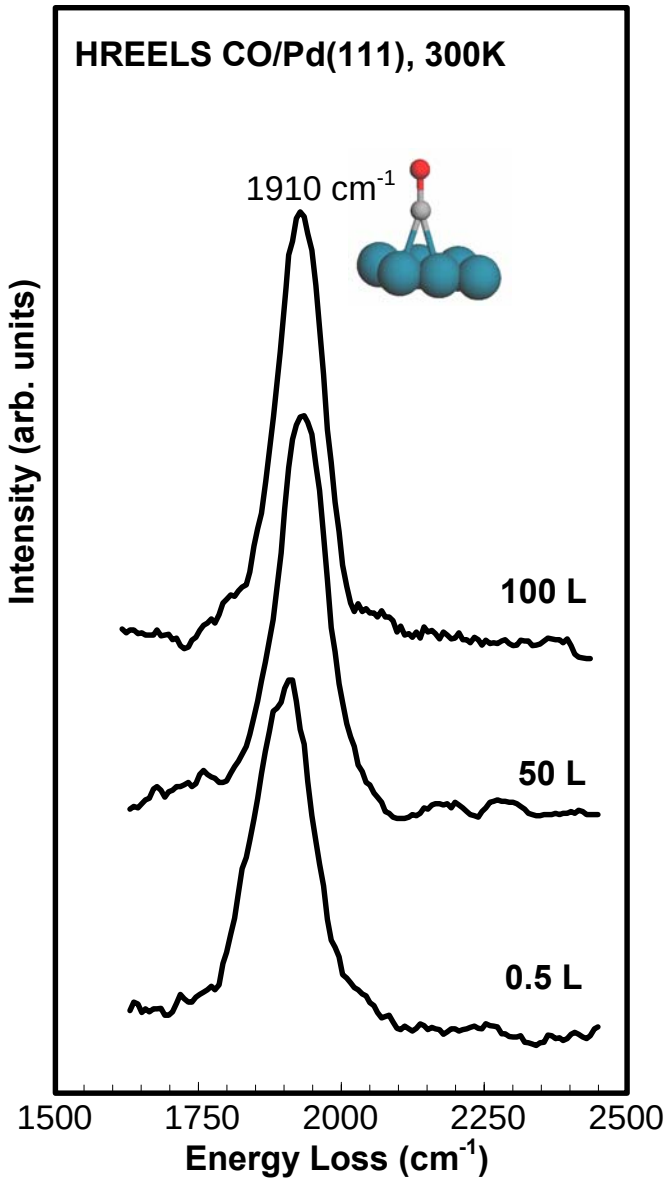

Figure 5. HREEL Spectra obtained after dosing different coverages of CO on Pd(111) at 300 K

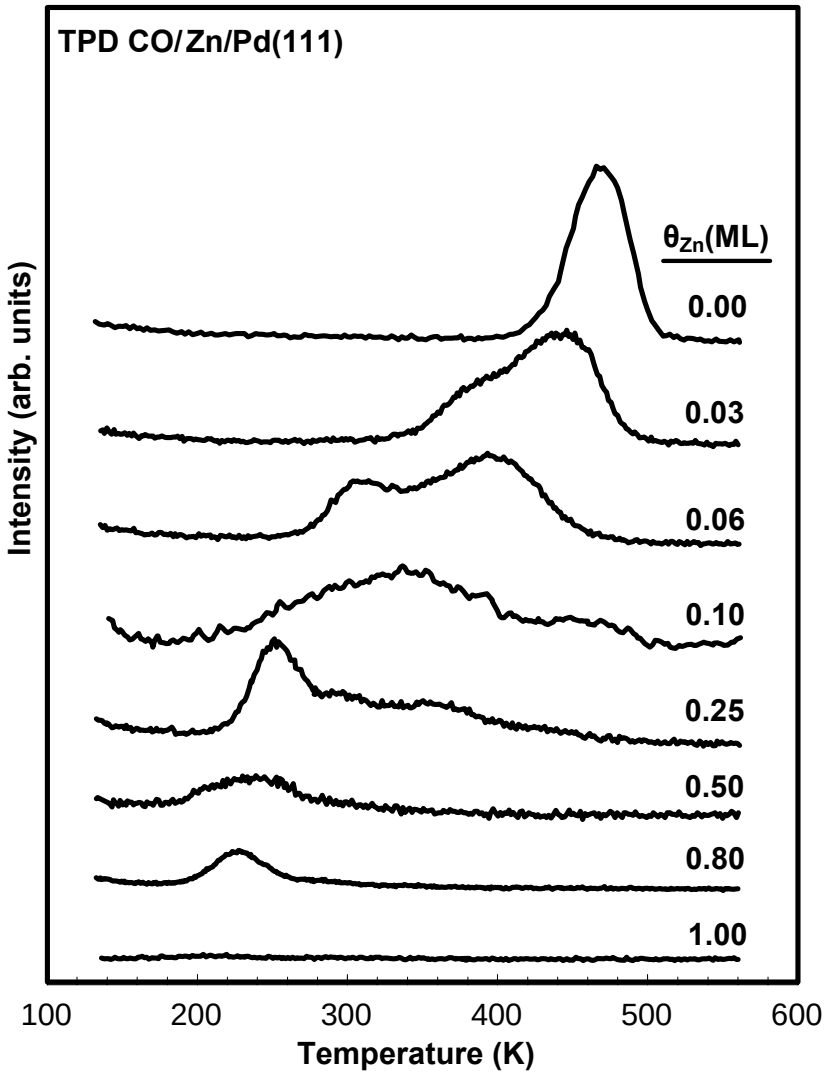

Figure 6. TPD data obtained after the exposure of 1/3 ML of CO onto 0 – 1 ML of Zn on Pd(111) at 100K.

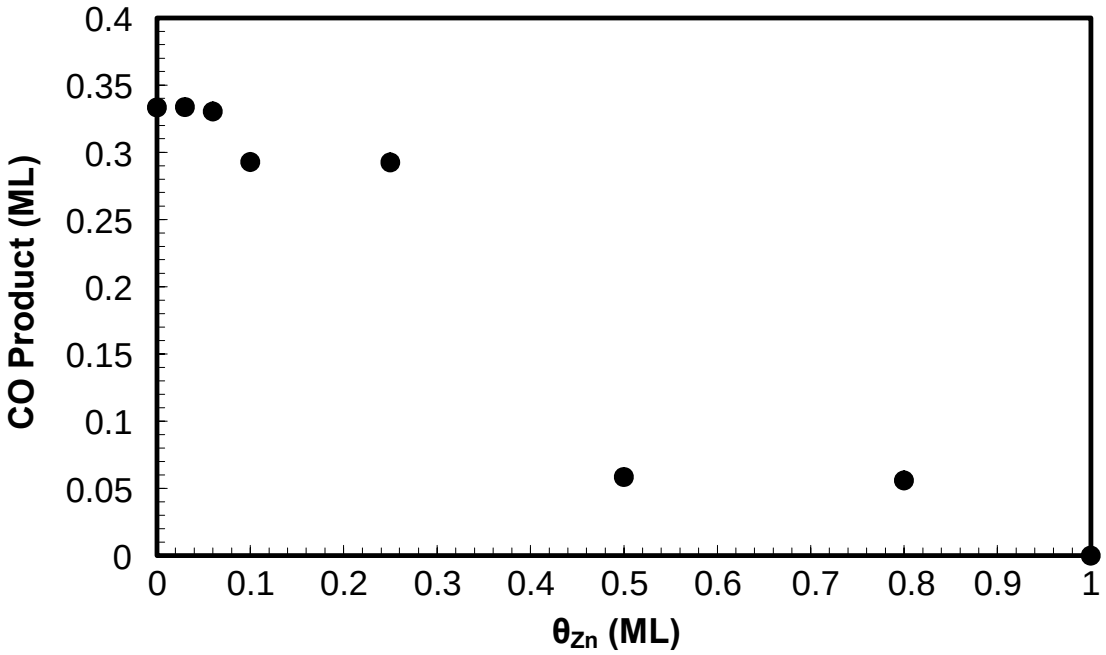

Figure 7. The total amount of adsorbed CO onto the Zn/Pd(111) as a function of the Zn coverage

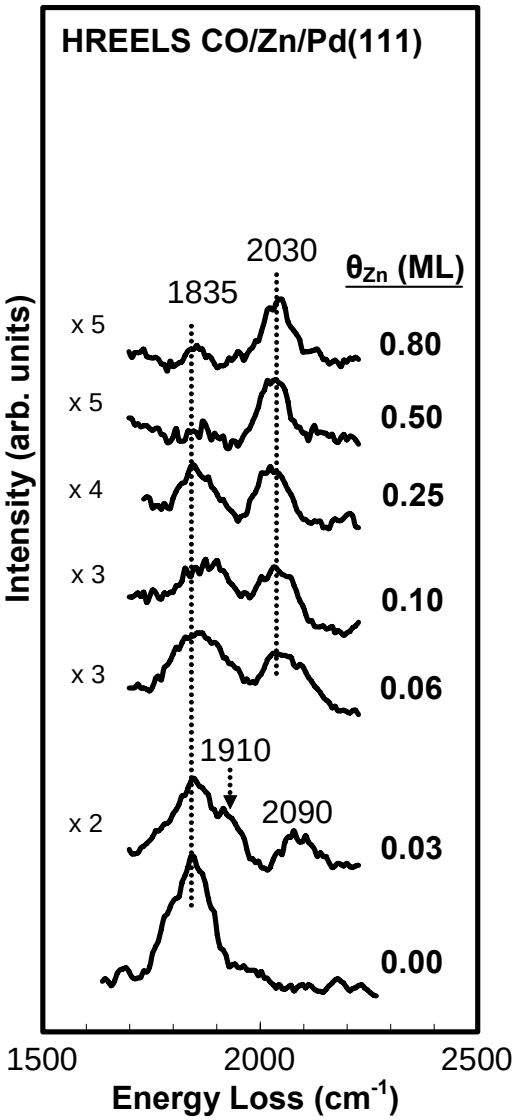

Figure 8. HREELS obtained after the exposure of 0.5 L of CO at 100 K on 0 – 0.8ML of Zn/Pd(111)

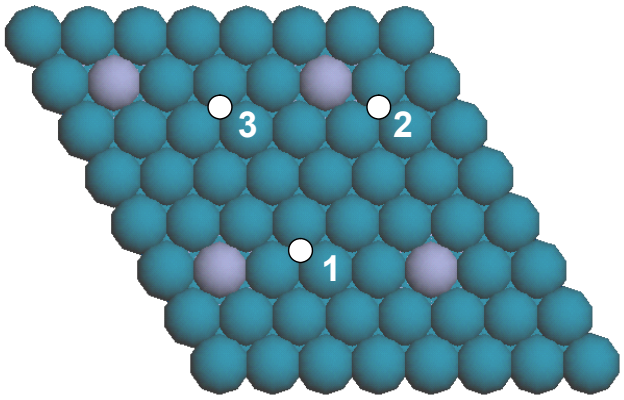

Figure 9. Model of 0.06 ML of Zn/Pd alloy surface showing three different types of three-fold hollow sites: (1) one Pd with a Zn nearest neighbor, (2) two Pd with Zn nearest neighbors and (3) no Pd with Zn next nearest neighbors

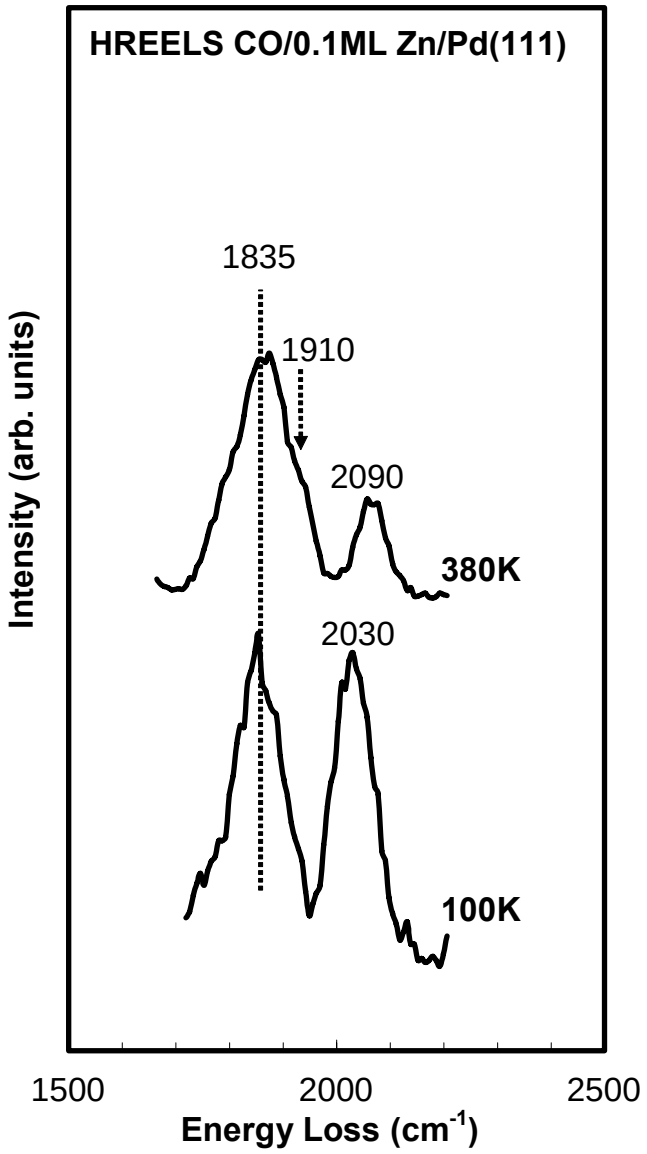

Figure 10. HREELS of 0.5 L of CO on 0.1 ML of Zn/Pd(111) obtained at 100 K after annealing to 100K and 380K

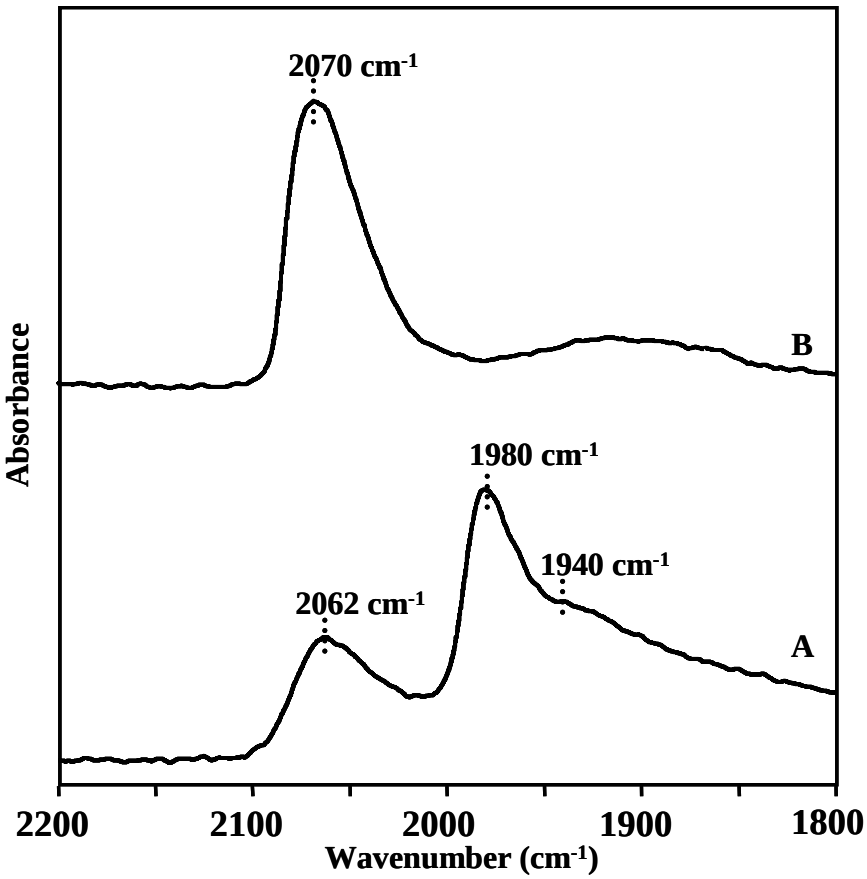

Figure 11. FTIR spectra of CO adsorbed on (A) $Pd/ZnO/Al_2O_3$, and (B) $PdZn/ZnO/Al_2O_3$. The spectra were collected at a sample temperature of 293 K.